



# 1 **Effects of ozone-vegetation coupling on surface ozone air** 2 **quality via biogeochemical and meteorological feedbacks**

3 Mehliyar Sadiq<sup>1</sup>, Amos P. K. Tai<sup>1,2</sup>, Danica Lombardozzi<sup>3</sup>, and Maria Val Martin<sup>4</sup>

4 <sup>1</sup>Graduate Division of Earth and Atmospheric Sciences, Faculty of Science, Chinese University of Hong Kong,  
5 Hong Kong

6 <sup>2</sup>Earth System Science Programme, Faculty of Science, Chinese University of Hong Kong, Hong Kong

7 <sup>3</sup>National Center for Atmospheric Research, Boulder, Colorado, USA

8 <sup>4</sup>Department of Chemical and Biological Engineering, University of Sheffield, Sheffield, UK

9 *Correspondence to:* Amos P. K. Tai (amostai@cuhk.edu.hk)

10

11 **Abstract.** Tropospheric ozone is one of the most hazardous air pollutants as it harms both human health and  
12 plant productivity. Foliage uptake of ozone via dry deposition damages photosynthesis and causes stomatal  
13 closure. These foliage changes could lead to a cascade of biogeochemical and biogeophysical effects that not  
14 only modulate the carbon cycle, regional hydrometeorology and climate, but also cause feedbacks onto surface  
15 ozone concentration itself. In this study, we implement a semi-empirical parameterization of ozone damage on  
16 vegetation in the Community Earth System Model to enable online ozone-vegetation coupling, so that for the  
17 first time ecosystem structure and ozone concentration can coevolve in fully coupled land-atmosphere  
18 simulations. With ozone-vegetation coupling, present-day surface ozone is simulated to be higher by up to 6  
19 ppbv over Europe, North America and China. Reduced dry deposition velocity following ozone damage  
20 contributes to ~40-100% of those increases, constituting a significant positive biogeochemical feedback on  
21 ozone air quality. Enhanced biogenic isoprene emission is found to contribute to most of the remaining  
22 increases, and is driven mainly by higher vegetation temperature that results from lower transpiration rate. This  
23 isoprene-driven pathway represents an indirect, positive meteorological feedback. The reduction in both dry  
24 deposition and transpiration is mostly associated with reduced stomatal conductance following ozone damage,  
25 whereas the modification of photosynthesis and further changes in ecosystem productivity (which are significant  
26 per se) are found to play a smaller role in contributing to the ozone-vegetation feedbacks. Our results highlight  
27 the need to consider two-way ozone-vegetation coupling in Earth system models to derive a more complete  
28 understanding and yield more reliable future predictions of ozone air quality.

29

## 30 **1 Introduction**

31 Tropospheric ozone is one of the air pollutants of the greatest concern due to its significant harm to  
32 human respiratory health. Increases of ozone since the preindustrial time have been associated with a global  
33 annual burden of  $0.7 \pm 0.3$  million respiratory mortalities (Anenberg et al., 2010). Decades of observational  
34 records have also demonstrated the damaging effect of surface ozone on vegetation and crop productivity  
35 (Ainsworth et al., 2012). The phytotoxicity of ozone is shown to induce stomatal closure and reduce primary  
36 production, with ramifications for climate through the modification of surface energy and water fluxes and a  
37 decrease in the land carbon sink (Sitch et al., 2007; Wittig et al., 2007; Lombardozzi et al., 2015). Meanwhile,  
38 vegetation helps reduce ambient ozone concentration through stomatal deposition (e.g., Kroeger et al., 2014).



39 However, the effect of such ozone-induced vegetation damage on ozone concentration itself, which thereby  
40 completes the ozone-vegetation feedback loop, has not been examined before but is potentially significant in  
41 modulating tropospheric ozone. This work uses a fully coupled land-atmosphere model to, for the first time,  
42 quantify the impacts of ozone-vegetation coupling on surface ozone, and diagnoses the contributions from  
43 various feedback pathways in terrestrial ecosystems.

44 Tropospheric ozone is mainly produced from the photochemical oxidation of carbon monoxide (CO),  
45 methane (CH<sub>4</sub>) and non-methane volatile organic compounds (VOCs) by hydroxyl radical (OH) in the presence  
46 of nitrogen oxides (NO<sub>x</sub> ≡ NO + NO<sub>2</sub>). Vegetation plays various significant roles modulating surface ozone  
47 concentration. Precursor gases of ozone have large anthropogenic and natural sources, including vegetation and  
48 soil microbes for CH<sub>4</sub> and other VOCs. The most abundant single non-methane VOC species emitted by  
49 vegetation is isoprene (C<sub>5</sub>H<sub>8</sub>), which acts as a major precursor for ozone formation in polluted, high-NO<sub>x</sub>  
50 regions, but eliminates ozone by direct ozonolysis or by sequestering NO<sub>x</sub> as isoprene nitrate in more pristine  
51 environments (Fiore et al., 2011). The major sinks for tropospheric ozone include photolysis in the presence of  
52 water vapor and uptake by vegetation (i.e., dry deposition, mainly through the leaf stomata). Vegetation,  
53 therefore, plays a significant role in modulating ozone biogeochemically through dry deposition and biogenic  
54 VOC emissions. Meanwhile, transpiration from vegetation can affect ozone by regulating the overlying  
55 hydrometeorological environment. For instance, transpiration influences near-surface water vapor content,  
56 which affects the chemical loss rate of ozone. Transpiration also controls surface temperature and mixing depth,  
57 which can all influence the formation and dilution of ozone in the atmospheric boundary layer (Jacob and  
58 Winner, 2009).

59 Vegetation not only affects but is also affected by surface ozone. Stomatal uptake of ozone by leaves  
60 damages internal plant tissues, leading to severe damage to forest, grassland and agricultural productivity  
61 (Ashmore, 2005; Karnosky et al., 2007; Ainsworth et al., 2012). Elevated ozone since the industrial revolution  
62 is suggested to have reduced light-saturated photosynthetic rate and stomatal conductance by 11% and 13%,  
63 respectively (Wittig et al., 2007). Modeling studies have also suggested that elevated ozone could decrease gross  
64 primary production (GPP) by 4-8% in the eastern US and more severely so (11-17%) in several hot spots there  
65 (Yue and Unger, 2014), and decrease transpiration rate globally by 2-2.4% (Lombardozi et al., 2015), with  
66 significant implications for climate. For instance, the ozone-induced reduction in the global land carbon sink is  
67 shown to have an indirect radiative forcing of +0.62-1.09 W m<sup>-2</sup>, which is comparable to the direct radiative  
68 forcing of ozone as a greenhouse gas (0.89 W m<sup>-2</sup>) and contributes to more pronounced warming (Sitch et al.,  
69 2007). Changes in stomatal conductance also modify the land-atmosphere exchange of water and energy and  
70 thus regional hydrometeorology (Bernacchi et al., 2011; Lombardozi et al., 2015). In view of the important  
71 roles vegetation plays in shaping tropospheric ozone, the above biogeochemical and biogeophysical effects  
72 induced by ozone damage would affect not only weather and climate but also constitute important feedbacks  
73 that ultimately affect ozone air quality itself.

74 In many land surface models, photosynthetic rate and stomatal conductance are highly coupled through  
75 the computation within the Farquhar/Ball-Berry model (Farquhar et al., 1980; Ball et al., 1987; Bonan et al.,  
76 2011). In global modeling studies on ozone-mediated vegetation changes and climate (Sitch et al., 2007; Collins  
77 et al., 2010; Yue and Unger, 2014), the effects of ozone damage on photosynthesis and stomata are thus strongly  
78 coupled to each other. Ozone uptake is assumed to directly affect photosynthetic rate, which in turn affects



79 stomatal conductance via changes in internal CO<sub>2</sub> concentration. However, recent studies have suggested that  
80 separate modification of photosynthetic rate and stomatal conductance by cumulative ozone uptake in the  
81 Community Land Model (CLM) leads to better representation of plant responses to ozone exposure  
82 (Lombardozzi et al., 2012). This decoupling of ozone effects on photosynthesis and stomata is shown to  
83 decrease water use efficiency of affected plants, but leads to an overall smaller impact of ozone on transpiration  
84 and GPP than previously predicted.

85 Many climate-chemistry-biosphere modeling studies performed to date have demonstrated the  
86 importance of the coevolution of climate, land cover and terrestrial ecosystems in air quality simulations and  
87 predictions (Wu et al., 2012; Tai et al., 2013; Pacifico et al., 2015), but they have not taken into account the  
88 potentially strong feedbacks arising from ozone damage on vegetation. For instance, ozone exposure can reduce  
89 stomatal conductance and thus transpiration rate, which may modify the partition between latent and sensible  
90 heat fluxes and lead to a cascade of meteorological changes, including lower humidity that reduces the chemical  
91 loss rate of ozone, a thicker boundary layer that dilutes all pollutants, and higher temperature that enhances  
92 ozone mainly through increased biogenic emissions and higher abundance of NO<sub>x</sub> (Jacob and Winner, 2009).  
93 These transpiration-mediated pathways can be characterized as biogeophysical feedbacks as are commonly  
94 known in the context of climate change, but here we prefer to call them simply “meteorological feedbacks” to  
95 emphasize that they are effected through ozone-induced changes in the meteorological variables that ultimately  
96 affect ozone. On the other hand, reduced dry deposition caused by lower stomatal conductance and a decline in  
97 leaf area index (LAI) following ozone exposure can potentially increase ozone. The short-term impact of ozone  
98 on foliage-level isoprene emission is still under debate (Fares et al., 2006; Calfapietra et al., 2007), but as  
99 vegetation density (e.g., represented by LAI) declines due to chronic ozone exposure (Yue et al., 2014), isoprene  
100 emission would likely decrease in the long term. These pathways directly involving plant biogeochemistry and  
101 atmospheric chemistry can be collectively termed “biogeochemical feedbacks”. Fig. 1 summarizes the  
102 potentially important biogeochemical and meteorological feedbacks on surface ozone concentration, which are  
103 expected to have ramifications for simulations and future projections of ozone air quality. Such feedbacks may  
104 further alter atmospheric composition (e.g., aerosol and oxidant concentrations) and climate at large but remain  
105 poorly characterized in an Earth system modeling framework.

106 In this study, we adopt and implement a semi-empirical scheme for ozone-induced vegetation damage  
107 (Lombardozzi et al., 2015) into a coupled land-atmosphere model with fully interactive atmospheric chemistry  
108 and biogeochemical cycles, and examine the resulting impacts on present-day simulations of tropospheric ozone  
109 air quality with respect to observations. We perform sensitivity simulations to quantify the relative importance  
110 of different biogeochemical and meteorological feedback pathways, elucidate the larger sources of uncertainties,  
111 and make specific suggestions regarding Earth system model development.

112

## 113 **2 Methods**

### 114 **2.1 Model description**

115 This study investigates the impacts of ozone-vegetation coupling on ozone concentrations using the  
116 Community Earth System Model (CESM), which includes several different model components representing the  
117 atmosphere, land, ocean, and sea ice to be run independently or in various coupled configurations (Oleson et al.,  
118 2010; Lamarque et al., 2012; Neale et al., 2013). We employ CESM version 1.2.2 with fully interactive



119 atmosphere and land components, but with prescribed ocean and sea ice consistent with the scenarios of  
 120 concern. For the atmosphere component, we use the Community Atmosphere Model version 4 (CAM4) (Neale  
 121 et al., 2013) fully coupled with an atmospheric chemistry scheme (i.e., CAM-Chem) that contains full  
 122 tropospheric O<sub>3</sub>-NO<sub>x</sub>-CO-VOC-aerosol chemistry based on the MOZART-4 chemical transport model (CTM)  
 123 (Emmons et al., 2010; Lamarque et al., 2012). The version of CAM-Chem simulates the concentrations of 56  
 124 atmospheric chemical species at a horizontal resolution of 1.9°×2.5° latitude-longitude and 26 vertical layers for  
 125 the atmosphere up to around 40 km.

126 For the land component, we use the Community Land Model version 4 (CLM4) (Oleson et al., 2010)  
 127 with active carbon-nitrogen biogeochemistry (CLM4CN), which contains prognostic treatment of terrestrial  
 128 carbon and nitrogen cycles (Lawrence et al., 2011). In CLM4, the Model of Emissions of Gases and Aerosols  
 129 from Nature (MEGAN) version 2.1 is used to compute biogenic emissions online as functions of changing LAI,  
 130 vegetation temperature, soil moisture and other environmental conditions (Guenther et al., 2012). For dry  
 131 deposition of gases and aerosols we use the resistance-in-series scheme in CLM4 as described in Lamarque et  
 132 al. (2012) with a further update of optimized coupling of stomatal resistance to LAI (Val Martin et al., 2014).  
 133 Evapotranspiration is calculated based on the Monin-Obukhov similarity theory and the diffusive flux-resistance  
 134 model with dependence on vegetation, ground and surface temperature, specific humidity, and an ensemble of  
 135 resistances that are functions of meteorological and land surface conditions (Oleson et al., 2010; Lawrence et al.,  
 136 2011; Bonan et al., 2011). Evapotranspiration is partitioned into transpiration, ground evaporation and canopy  
 137 evaporation, with updates from Lawrence et al. (2011), and is linked to photosynthesis via the computation of  
 138 stomatal resistance, as described below.

139

## 140 2.2 Photosynthesis- stomatal conductance model and ozone damage parameterization

141 The Farquhar/Ball-Berry model is used in CLM4CN to compute leaf-level photosynthetic rate and  
 142 stomatal conductance under different environmental conditions (Farquhar et al., 1980; Ball et al., 1987). Leaf  
 143 photosynthetic rate,  $A$  ( $\mu\text{mol CO}_2 \text{ m}^{-2} \text{ s}^{-1}$ ), is calculated as

$$144 A = \min(W_c, W_j, W_e) \quad (1)$$

145 where  $W_c$  is the Ribulose-1,5-bisphosphate carboxylase (RuBisCO)-limited rate of carboxylation,  $W_j$  is the light-  
 146 limited rate, and  $W_e$  is the export-limited rate is  $W_e$ . Photosynthesis and stomatal conductance ( $g_s$ ) are related by

$$147 g_s = \frac{1}{r_s} = m \frac{A}{c_s e_i} P_{\text{atm}} + b \quad (2)$$

148 where  $g_s$  is the leaf stomatal conductance;  $r_s$  is the leaf stomatal resistance ( $\text{s m}^2 \mu\text{mol}^{-1}$ );  $m$  is the slope of the  
 149 conductance-photosynthesis relationship with values ranging from 5 to 9;  $c_s$  is the CO<sub>2</sub> partial pressure at leaf  
 150 surface (Pa);  $e_s$  is the vapor pressure at leaf surface (Pa);  $e_i$  is the saturation vapor pressure inside the leaf (Pa);  
 151  $P_{\text{atm}}$  is the atmospheric pressure (Pa); and  $b$  is the minimum stomatal conductance when  $A = 0$ , and is set to give  
 152 a maximum stomatal resistance of 20000  $\text{s m}^{-1}$  in CLM4 (Oleson et al., 2010).

153 Parameterization for the impact of ozone exposure on photosynthesis and stomatal conductance follows  
 154 the work of Lombardozi et al., (2015), who tested the sensitivity of global ecosystem productivity and  
 155 hydrometeorology to ozone damage on vegetation using satellite phenology (i.e., prescribed LAI, canopy height,  
 156 etc.) and present-day ozone concentrations. The scheme uses two sets of ozone impact factors, one for  
 157 modifying photosynthetic rate and another for stomatal conductance independently. These factors account for  
 158 different plant groups, and are calculated based on the cumulative ozone uptake (CUO) under different levels of



159 chronic ozone exposure (Lombardozzi et al., 2013). CUO integrates ozone flux into leaves over the growing  
160 season as

$$161 \quad \text{CUO} = \sum(k_{\text{O}_3} / r_s) [\text{O}_3] \quad (3)$$

162 where  $[\text{O}_3]$  is the surface ozone concentration computed from CAM-Chem in every time step, and  $k_{\text{O}_3}$  is the  
163 ratio of leaf resistance to ozone to leaf resistance to water. Ozone uptake is only cumulated during the growing  
164 season when vegetation is the most vulnerable to air pollution episodes; growing season is defined as the period  
165 in which total leaf area index (TLAI)  $> 0.5$  (Lombardozzi et al., 2012). Ozone uptake only cumulates when the  
166 ozone flux is above a critical threshold,  $0.8 \text{ nmol O}_3 \text{ m}^{-2} \text{ s}^{-1}$ , to account for ozone detoxification by vegetation at  
167 lower ozone levels (Lombardozzi et al., 2015). Three different plant groups are accounted for: evergreen,  
168 deciduous, and crops/grasses. The ozone impact factors have empirical linear relationships with CUO such that

$$169 \quad F_{p\text{O}_3} = a_p \times \text{CUO} + b_p \quad (4)$$

$$170 \quad F_{c\text{O}_3} = a_c \times \text{CUO} + b_c \quad (5)$$

171 where  $F_{p\text{O}_3}$  is the ozone damage factor multiplied to the photosynthesis rate ( $A$ ), and  $a_p$  and  $b_p$  are slope and  
172 intercept from empirical and experimental studies (listed in Table 1);  $F_{c\text{O}_3}$  is the ozone damage factor multiplied  
173 to stomatal conductance ( $g_s$ ), and  $a_c$  and  $b_c$  are the corresponding slope and intercept (Table 1). The ozone  
174 damage is applied to the optimal photosynthesis and stomatal conductance values, which are calculated  
175 iteratively first without ozone damage, to allow the damage to be applied independently.

176

### 177 **2.3 Model experiments**

178 Incorporating the ozone-vegetation parameterization above into CLM4CN and coupling it with CAM-  
179 Chem, we allow, for the first time, ecosystem structure (e.g., in terms of LAI and canopy height) to evolve in  
180 response to ozone exposure but at the same time allow ozone concentration to evolve in response to such  
181 ecosystem changes. Therefore, online ozone-vegetation coupling and feedback are included. We conduct four  
182 sets of fully coupled land-atmosphere simulations: 1) a control case without ozone damage on vegetation  
183 ([CTR]); 2) simulation with both photosynthetic rate and stomatal conductance modified by ozone impact  
184 factors (independently) ([PHT+COND]), following the approach of Lombardozzi et al (2015); 3) simulation  
185 where we apply the ozone impact factor to photosynthetic rate only ([PHT]), but stomatal conductance is  
186 calculated using the intact, optimal photosynthetic rate; and 4) simulation where we apply the ozone impact  
187 factor to stomatal conductance only ([COND]), but photosynthetic rate is calculated using the intact stomatal  
188 conductance. Simulations [PHT] and [COND], when compared with [PHT+COND], allow us to quantify the  
189 relative contribution from each pathway. To determine the relative contribution of those pathways involving  
190 biogenic emissions toward the overall ozone-vegetation feedback, we conduct an additional set of sensitivity  
191 simulations with prescribed isoprene emission and MEGAN turned off: a control case with no MEGAN  
192 (CTR\_nM), and a simulation with modified photosynthesis and stomatal conductance but with no MEGAN  
193 ([PHT+COND\_nM]). To determine the relative contribution of pathways involving dry deposition vs.  
194 transpiration, we compare simulated results with that of Val Martin et al. (2014) who have used the similar



195 CAM-Chem-CLM framework but without ozone-vegetation coupling to test the sensitivity of ozone to  
196 perturbations in dry deposition velocity.

197 All simulations are conducted for 20 years using year 2000 initial conditions and the corresponding  
198 land cover data (e.g., land cover and land use types, satellite LAI, etc.). The first five years of outputs are treated  
199 as spin-up and thus discarded in the analysis. We observe that the annual averages of key aboveground  
200 ecosystem parameters such as LAI and ozone concentration come into a relatively steady state after 5 years. We  
201 focus on changes in the 15-year northern summertime (JJA) averages for most of the variables in the rest of this  
202 paper because this is the period when the growing season of the majority of global vegetation overlaps most  
203 significantly with high-ozone season especially in the northern midlatitudes.

204

### 205 **3 Simulated ozone with and without ozone-vegetation coupling**

206 Figure 2(a) shows the 15-year mean summertime surface ozone concentration from the [PHT+COND]  
207 simulation. The corresponding cumulative ozone uptake (CUO) used to affect vegetation is shown in Fig. 2(b).  
208 Simulated ozone is generally higher in the northern midlatitudes than elsewhere, and is the highest over the  
209 Mediterranean where solar radiation is particularly strong. CUO also has high values in Europe, but the overall  
210 distribution does not exactly follow that of surface ozone concentration because CUO also depends on the  
211 length of the growing season and stomatal conductance. CUO ranges between 20-70 mmol m<sup>-2</sup> over regions  
212 with both high summertime ozone and high productivity. The simulated CUO is comparable in both magnitude  
213 and spatial distribution with Lombardozzi et al., (2015), who used prescribed meteorology, ozone and  
214 vegetation phenology with no active carbon-nitrogen cycle or atmospheric coupling, as opposed to this study.  
215 This suggests that online ozone-vegetation coupling, which can modify ozone concentration substantially  
216 depending on the region, lead to a similar pattern of ozone damage on vegetation to the case using prescribed  
217 ozone. During the growing season, CUO is used to calculate the ozone impact factors that modify  
218 photosynthetic rate and stomatal conductance according to Eq. (4) and (5) and parameter values listed in Table  
219 1.

220 Figure 3 shows the differences in surface ozone concentration in different simulations from the control  
221 case. Implementing ozone-vegetation coupling that includes simultaneous modification of photosynthetic rate  
222 and stomatal conductance by ozone exposure (the [PHT+COND] case) increases mean surface ozone globally,  
223 and significant increases by up to 4-6 ppbv are found over China, North America and Europe (Fig. 3a). Ozone  
224 exposure is thus found to constitute a positive feedback loop via vegetation that ultimately enhances surface  
225 ozone levels when ozone-vegetation coupling is accounted for.

226 The simulated increases in ozone levels due to ozone-vegetation coupling are significant when  
227 compared with the possible impacts of 2000-2050 climate and land cover changes on surface ozone, which are  
228 in the range of +1-10 ppbv (Jacob & Winner, 2009; Tai et al., 2013; Val Martin et al., 2015). These simulated  
229 increases, however, slightly worsen the performance of CAM-Chem in reproducing ozone concentrations  
230 against observations as seen in Fig. 4, which shows the model-observation comparison for the control case  
231 (standard CAM-Chem-CLM with dry deposition improvement of Val Martin et al. (2014)) and the  
232 [PHT+COND] case. The high-biases in CESM-simulated summertime surface ozone concentrations in North  
233 America and Europe are a commonly acknowledged issue with CAM-Chem (Lamarque et al., 2012) and other  
234 global and regional models (Lapina et al., 2014; Parrish et al., 2014). Inclusion of ozone-vegetation coupling in



235 the model further increases the normalized mean biases of the modeled results against three sets of observational  
236 data: Clean Air Status and Trends Network (CASTNET) (1999-2001), Air Quality System (AQS) (1999-2001),  
237 and European Monitoring and Evaluation Programme (EMEP) (1999-2001), from 18% to 22%, 31% to 35%,  
238 14% to 22%, respectively. Given the sound theoretical and empirical basis of ozone damage on vegetation, this  
239 further highlights the urgency to revise other model processes and modules relevant for ozone simulations.

240

#### 241 **4 Attribution to different biogeochemical and meteorological feedback pathways**

242 Figures 3(b) and 3(c) show the differences in ozone for the cases where ozone damages stomatal  
243 conductance alone and photosynthesis alone, respectively, noting that each of them is calculated using the  
244 undamaged, intact values of the other variable. Comparison of Fig. 3(a) with (b)-(c) shows that the modification  
245 of stomatal conductance by ozone uptake contributes more dominantly to the overall effect of ozone-vegetation  
246 coupling (Fig. 3a). This suggests that, among the various feedback pathways that may influence surface ozone  
247 (Fig. 1), those triggered by changes in stomatal conductance are generally more important than those associated  
248 with photosynthesis or the associated changes in ecosystem production and structure including LAI, at least in  
249 the modeling framework of this study. This is also supported by sensitivity simulations performed under the  
250 same modeling framework but without ozone damage, in which a 50% of increase in LAI decreases  
251 summertime surface ozone by on average 3 ppb, which is relatively small in comparison with the changes  
252 following optimization of stomatal resistance (Val Martin et al., 2014). Indeed, the effect of modifying stomatal  
253 conductance alone ([COND]; Fig. 3b) is slightly larger than the case of [PHT+COND] (Fig. 3a), where the  
254 additional effect of modifying photosynthesis together with stomatal conductance would slightly offset the  
255 overall positive feedback on ozone. It is noteworthy that this additional effect is, however, not consistent with  
256 the effect of modifying photosynthesis alone ([PHT]; Fig. 3c), reflecting nonlinear interactions between  
257 photosynthesis and stomatal conductance.

258 Figure 5 shows the differences in dry deposition velocity, transpiration rate and biogenic isoprene  
259 emission between the [PHT+COND] and [CTR] simulations. Over China, Europe and North America, ozone  
260 dry deposition velocity is lower (by up to ~20%) in [PHT+COND]. In these same regions but especially in the  
261 eastern US, southern Europe and southern China, isoprene emission is significantly higher (by up to ~50%). In  
262 addition, in similar regions but especially in central North America, the transpiration rate is reduced by ozone  
263 exposure (by up to ~20%), which would reduce boundary-layer humidity, increase surface temperature, enhance  
264 dry convection and thicken the boundary layer. In view of Fig. 1, all of these pathways may add to or offset each  
265 other, leading to the overall ozone changes seen in Fig. 3(a). The sensitivity simulations and comparison with  
266 Val Martin et al. (2014), which examined the sensitivity of simulated ozone to differences in dry deposition  
267 schemes under essentially the same modeling framework, allow us to quantify more precisely which of these  
268 pathways are more important as we discuss next.

269 Figure 6(a) shows the changes in surface ozone in the [PHT+COND\_nM] minus CTR\_nM simulations,  
270 where we use prescribed biogenic emissions from the original control case (CTR) to drive ozone chemistry so  
271 that we essentially shut down any feedback pathways involving biogenic emissions. A comparison between Fig.  
272 6(a) and Fig. 3(a) shows that the changes in biogenic isoprene emissions account for ~0-60% of the ozone  
273 increases over Europe, North America and China, while dry deposition and/or transpiration-driven  
274 meteorological changes (excluding the temperature effect on isoprene emission) account for remaining ~40-



275 100%. We further show in Fig. 6(b) the theoretical changes in surface ozone by multiplying the dry deposition  
276 changes in Fig 5(a) by the change in ozone concentration per unit change in dry deposition velocity from the  
277 study of Val Martin et al. (2014). We find that the ozone changes in Fig. 6(a) and Fig. 6(b) are similar in  
278 magnitude, suggesting that globally most of the non-isoprene-driven differences in ozone is driven by dry  
279 deposition. Notable exceptions include the US Midwest and southeastern Europe, where higher mixing depth  
280 following reduced transpiration might have partly offset the ozone positive feedback; and western Europe,  
281 where the lower chemical loss rate following reduced transpired water might have further enhanced the positive  
282 feedback.

283 The simulated general reduction in dry deposition velocity and transpiration rate (Fig. 5a and 5b) is  
284 mostly due to increased stomatal resistance (Fig. 7a), i.e., reduced stomatal conductance, a direct response to  
285 cumulative ozone uptake. The reduced dry deposition represents a positive biogeochemical feedback on ozone  
286 (orange arrows in Fig. 1). The simulated increase in biogenic isoprene emission (Fig. 5c) is found to be mostly  
287 driven by higher surface (thus vegetation) temperature (Fig. 7b) that results from lower transpiration rate and  
288 latent heat flux (Fig. 7c). Therefore, this feedback loop involving biogenic emissions is indeed an indirect,  
289 meteorological feedback that is also initiated by stomatal and transpiration changes (purple arrows in Fig. 1).

290 By including immediate ozone-vegetation coupling, we find a larger decline in transpiration rate (6.4%  
291 globally) than in the offline, uncoupled land model results (2.0-2.4%) estimated by Lombardozzi et al. (2015).  
292 On the other hand, although reduced photosynthesis and the resulting long-term changes in GPP and LAI (Fig.  
293 7d-e) play a smaller role than reduced stomatal conductance in shaping simulated ozone (Fig. 3b-c), the impacts  
294 are not negligible (up to 3 ppb), especially as these changes are also nonlinearly coupled to stomatal changes.  
295 Photosynthetic rate decreases by up to 20% directly due to the ozone effect (Fig. 7f), which is quite similar both  
296 in magnitude and spatial pattern to the results of Lombardozzi et al. (2015), but the corresponding GPP and LAI  
297 changes are relatively small (~5% over regions concerned), likely reflecting the relaxation of nitrogen limitation  
298 when photosynthesis is reduced. Grid-level GPP and LAI in certain areas increase despite reduced leaf-level  
299 photosynthetic rate, likely reflecting more carbon allocation to leaves to compensate the reduced photosynthetic  
300 rate, relaxation of nitrogen limitation, and enhanced vegetation temperature following reduced transpiration.

301

## 302 5 Conclusions and discussion

303 Tropospheric ozone is one of the most hazardous air pollutants due to its harmful effects on human health  
304 and damage to forest and agricultural productivity. Stomatal uptake of ozone by leaves reduces both  
305 photosynthetic rate and stomatal conductance. These vegetation changes can induce a cascade of  
306 biogeochemical and biogeophysical (or meteorological) effects (Fig. 1) that ultimately modulate climate, carbon  
307 cycle and also feedback onto ozone air quality itself. The direct, biogeochemical feedback pathways include  
308 reduced ozone dry deposition and biogenic VOC emissions. The indirect, meteorological feedback pathways are  
309 facilitated by transpiration-driven changes in the meteorological environment that influence ozone formation  
310 and removal. Many land surface modeling studies have estimated the direct effects of ozone on ecosystem  
311 production and land-atmosphere water exchange (Yue and Unger, 2014; Lombardozzi et al., 2015), and  
312 predicted a possible positive radiative forcing from the ozone-induced decline in the land-carbon sink (Sitch et  
313 al., 2007). However, the potentially large feedback effects onto ozone concentration itself have not been  
314 examined, which may have further ramifications for climate forcing because of the greenhouse effect of ozone.





315           In this study, we implement a semi-empirical parameterization of ozone damage on vegetation  
316 (Lombardozzi et al., 2015) into the CESM (CAM4-Chem-CLM4CN) modeling framework to enable online  
317 ozone-vegetation coupling so that vegetation variables can evolve in response to ozone exposure, and at the  
318 same time simulated ozone concentration can respond to ecosystem changes. Our scheme modifies leaf-level  
319 photosynthesis and stomatal conductance separately via the ozone impact factors, which are assumed to have  
320 empirical linear relationships with cumulative ozone uptake and account for different plant groups. Sensitivity  
321 simulations are conducted to determine the relative importance of different feedback pathways.

322           With ozone-vegetation coupling, surface ozone is simulated to be higher by up to 6 ppbv over Europe,  
323 North America and China. This coupling effect is significant in view of the 2000-2050 effects of climate and  
324 land cover changes on surface ozone (+1-10 ppbv) as found in previous work (Jacob and Winner, 2009; Tai et  
325 al., 2013), and should be considered in future air quality projection studies. Reduced dry deposition velocity  
326 following the modification contributes to ~40-100% and enhanced biogenic isoprene emission contributes to ~0-  
327 60% of the higher ozone concentrations. The dry deposition-driven ozone increases (by up to 4 ppbv) arise  
328 mostly from reduced stomatal conductance, and are consistent with the sensitivity of ozone to perturbations in  
329 dry deposition velocity found by Val Martin et al. (2014). This pathway constitutes a significant positive  
330 biogeochemical feedback on surface ozone. The other major feedback associated with enhanced isoprene  
331 emission is mostly driven by higher vegetation temperature that results from lower transpiration rate. This  
332 pathway constitutes an indirect, positive meteorological feedback on surface ozone. Depending on the region,  
333 transpiration-driven meteorological changes such as lower humidity and deeper mixing depth may also  
334 influence surface ozone. Transpiration rate is simulated to decrease by 6.4% globally, which is a larger change  
335 compared with the decrease estimated by Lombardozzi et al. (2015) and suggests an augmented effect due to the  
336 coupling between the atmosphere and ecosystems.

337           Modification of photosynthesis and further long-term changes in ecosystem productivity and structure,  
338 including LAI changes, are found to play a smaller role in contributing to the ozone-vegetation feedbacks than  
339 direct stomatal changes, but are not insignificant (up to +3 ppbv). The simulated changes in LAI (less than 5%)  
340 in this study are similar in magnitude to that by Yue et al. (2015), who included an active carbon cycle though  
341 using Yale Interactive terrestrial Biosphere (YIBs) model with a different ozone-vegetation parameterization.  
342 However, prognostic treatment of the carbon cycle and LAI calculation in CLM4CN are still known to be  
343 problematic, with large uncertainties and biases in the estimation of global carbon fluxes (Sun et al., 2012),  
344 arising from incomplete model parameterization and from uncertainty in photosynthetic parameters (Bonan et  
345 al., 2011). It is not surprising that changes in GPP as simulated here do not replicate the results of Lombardozzi  
346 et al. (2015), in which vegetation phenology is prescribed and the carbon and nitrogen cycles are not active  
347 (CLM4.5SP). Implementing ozone damage on vegetation in a model with more sophisticated and realistic  
348 representation of prognostic carbon-nitrogen cycle is highly warranted, so that the possible effects of ozone-  
349 induced long-term ecosystem changes can be examined more fully.

350           Large variability in the responses of different plants to ozone leads to considerable uncertainties in any  
351 global-scale studies (Lombardozzi et al., 2013). The model results could be improved with more detailed plant-  
352 type-specific ozone damage parameterization, including better estimates of plant vulnerability to ozone that will  
353 help refine the ozone uptake thresholds (Lombardozzi et al., 2015). An important caveat of this study is the  
354 consideration of only three plant groups to generalize the responses of global vegetation to ozone exposure



355 because data are largely unavailable for other plant groups. Another potential caveat is the uncertainty and lack  
356 of cross-validation in hydrometeorological simulations with respect to the ozone phytotoxicity scheme we  
357 newly implement, as we only focus on vegetation and atmospheric chemical changes in this study. Although  
358 most simulated vegetation variables are consistent with previous work, the changes in simulated vegetation  
359 temperature from ozone-vegetation coupling are not small (by up to +2°C) (Fig. 7b) and they result in quite  
360 substantial changes in isoprene emission, suggesting the need for further tuning of hydrometeorological processes  
361 in the model. In general, we have the highest confidence in the quantification of the biogeochemical pathway  
362 via stomata-driven deposition changes, which is straightforward and accounts for the majority of the ozone-  
363 vegetation feedbacks. On the other hand, the meteorological feedbacks introduce strong nonlinearity in the  
364 interactions between atmospheric chemistry and vegetation that is more difficult to isolate and understand.  
365 Parameterizing the ozone-vegetation coupling in a standalone chemical transport model with prescribed  
366 meteorology could be particularly helpful to more confidently separate between the effects of biogeochemical  
367 vs. meteorological feedbacks. This knowledge will be important in projecting the impacts of future climate and  
368 land cover changes on ozone air quality and climate feedbacks in the coming decades.

369

#### 370 **Acknowledgment**

371 This work was supported by the Early Career Scheme (Project #: 24300614) of the Research Grants  
372 Council of Hong Kong given to the principal investigator, Amos P. K. Tai. We also thank the Information  
373 Technology Services Centre (ITSC) at The Chinese University of Hong Kong for their devotion in providing the  
374 necessary computational services for this work.

375

#### 376 **References**

- 377 Ainsworth, E. A., Yendrek, C. R., Sitch, S., Collins, W. J., and Emberson, L. D.: The Effects of Tropospheric  
378 Ozone on Net Primary Productivity and Implications for Climate Change, *Annu Rev Plant Biol*, 63, 637-661,  
379 doi: 10.1146/annurev-arplant-042110-103829, 2012.
- 380 Anenberg, S. C., Horowitz, L. W., Tong, D. Q., and West, J. J.: An Estimate of the Global Burden of  
381 Anthropogenic Ozone and Fine Particulate Matter on Premature Human Mortality Using Atmospheric  
382 Modeling, *Environ Health Persp*, 118, 1189-1195, doi:10.1289/ehp.0901220, 2010.
- 383 Ashmore, M. R.: Assessing the future global impacts of ozone on vegetation, *Plant Cell Environ*, 28, 949-964,  
384 doi:10.1111/J.1365-3040.2005.01341.X, 2005.
- 385 Ball, J. T., Woodrow, I. E., and Berry, J. A.: A model predicting stomatal conductance and its contribution to  
386 the control of photosynthesis under different environmental conditions, in: *Progress in photosynthesis research*,  
387 Springer, 221-224, 1987.
- 388 Bernacchi, C. J., Leakey, A. D. B., Kimball, B. A., and Ort, D. R.: Growth of soybean at future tropospheric  
389 ozone concentrations decreases canopy evapotranspiration and soil water depletion, *Environ Pollut*, 159, 1464-  
390 1472, doi:10.1016/j.envpol.2011.03.011, 2011.
- 391 Bonan, G. B.: Forests and climate change: Forcings, feedbacks, and the climate benefits of forests, *Science*, 320,  
392 1444-1449, doi:10.1126/science.1155121, 2008.
- 393 Bonan, G. B., Lawrence, P. J., Oleson, K. W., Levis, S., Jung, M., Reichstein, M., Lawrence, D. M., and  
394 Swenson, S. C.: Improving canopy processes in the Community Land Model version 4 (CLM4) using global



- 395 flux fields empirically inferred from FLUXNET data, *J Geophys Res-Bioge*, 116, G02014,  
396 doi:10.1029/2010jg001593, 2011.
- 397 Calfapietra, C., Wiberley, A. E., Falbel, T. G., Linskey, A. R., Mugnozza, G. S., Karnosky, D. F., Loreto, F.,  
398 and Sharkey, T. D.: Isoprene synthase expression and protein levels are reduced under elevated O<sub>3</sub> but not  
399 under elevated CO<sub>2</sub> (FACE) in field-grown aspen trees, *Plant Cell Environ*, 30, 654-661, doi:10.1111/j.1365-  
400 3040.2007.01646.x, 2007.
- 401 Collins, W. J., Sitch, S., and Boucher, O.: How vegetation impacts affect climate metrics for ozone precursors, *J*  
402 *Geophys Res-Atmos*, 115, D23308, doi:10.1029/2010jd014187, 2010.
- 403 Emmons, L. K., Walters, S., Hess, P. G., Lamarque, J. F., Pfister, G. G., Fillmore, D., Granier, C., Guenther, A.,  
404 Kinnison, D., Laepple, T., Orlando, J., Tie, X., Tyndall, G., Wiedinmyer, C., Baughcum, S. L., and Kloster, S.:  
405 Description and evaluation of the Model for Ozone and Related chemical Tracers, version 4 (MOZART-4),  
406 *Geosci Model Dev*, 3, 43-67, 2010.
- 407 Fares, S., Barta, C., Brilli, F., Centritto, M., Ederli, L., Ferranti, F., Pasqualini, S., Reale, L., Tricoli, D., and  
408 Loreto, F.: Impact of high ozone on isoprene emission, photosynthesis and histology of developing *Populus alba*  
409 leaves directly or indirectly exposed to the pollutant, *Physiol Plantarum*, 128, 456-465, doi: 10.1111/j.1399-  
410 3054.2006.00750.x, 2006.
- 411 Farquhar, G. D., Caemmerer, S. V., and Berry, J. A.: A Biochemical-Model of Photosynthetic Co<sub>2</sub> Assimilation  
412 in Leaves of C-3 Species, *Planta*, 149, 78-90, doi:10.1007/Bf00386231, 1980.
- 413 Fiore, A. M., Levy, H., and Jaffe, D. A.: North American isoprene influence on intercontinental ozone pollution,  
414 *Atmos Chem Phys*, 11, 1697-1710, doi:10.5194/acp-11-1697-2011, 2011.
- 415 Gauss, M., Myhre, G., Pitari, G., Prather, M. J., Isaksen, I. S. A., Bernsten, T. K., Brasseur, G. P., Dentener, F.  
416 J., Derwent, R. G., Hauglustaine, D. A., Horowitz, L. W., Jacob, D. J., Johnson, M., Law, K. S., Mickley, L. J.,  
417 Muller, J. F., Plantevin, P. H., Pyle, J. A., Rogers, H. L., Stevenson, D. S., Sundet, J. K., van Weele, M., and  
418 Wild, O.: Radiative forcing in the 21st century due to ozone changes in the troposphere and the lower  
419 stratosphere, *J Geophys Res-Atmos*, 108, 4292, doi:10.1029/2002jd002624, 2003.
- 420 Guenther, A. B., Jiang, X., Heald, C. L., Sakulyanontvittaya, T., Duhl, T., Emmons, L. K., and Wang, X.: The  
421 Model of Emissions of Gases and Aerosols from Nature version 2.1 (MEGAN2.1): an extended and updated  
422 framework for modeling biogenic emissions, *Geosci Model Dev*, 5, 1471-1492, doi:10.5194/gmd-5-1471-2012,  
423 2012.
- 424 Herbinger, K., Then, C., Haberer, K., Alexou, M., Low, M., Remele, K., Rennenberg, H., Matyssek, R., Grill,  
425 D., Wieser, G., and Tausz, M.: Gas exchange and antioxidative compounds in young beech trees under free-air  
426 ozone exposure and comparisons to adult trees, *Plant Biology*, 9, 288-297, doi:10.1055/s-2006-924660, 2007.
- 427 Jacob, D. J., & Winner, D. A.: Effect of climate change on air quality, *Atmos Environ*, 43(1), 51-63,  
428 doi:10.1016/j.atmosenv.2008.09.051
- 429 Karnosky, D. F., Skelly, J. M., Percy, K. E., and Chappelka, A. H.: Perspectives regarding 50 years of research  
430 on effects of tropospheric ozone air pollution on US forests, *Environ Pollut*, 147, 489-506,  
431 doi:10.1016/j.envpol.2006.08.043, 2007.
- 432 Kroeger, T., Escobedo, F. J., Hernandez, J. L., Varela, S., Delphin, S., Fisher, J. R., & Waldron, J. (2014).  
433 Reforestation as a novel abatement and compliance measure for ground-level ozone. Proceedings of the  
434 National Academy of Sciences, 111(40), E4204-E4213, doi:10.1073/pnas.1409785111.



- 435 Lamarque, J. F., Emmons, L. K., Hess, P. G., Kinnison, D. E., Tilmes, S., Vitt, F., Heald, C. L., Holland, E. A.,  
436 Lauritzen, P. H., Neu, J., Orlando, J. J., Rasch, P. J., and Tyndall, G. K.: CAM-chem: description and evaluation  
437 of interactive atmospheric chemistry in the Community Earth System Model, *Geosci Model Dev*, 5, 369-411,  
438 doi:10.5194/gmd-5-369-2012, 2012.
- 439 Lapina, K., Henze, D. K., Milford, J. B., Huang, M., Lin, M., Fiore, A. M., ... & Bowman, K. (2014).  
440 Assessment of source contributions to seasonal vegetative exposure to ozone in the US. *Journal of Geophysical*  
441 *Research: Atmospheres*, 119(1), 324-340, doi: 10.1002/2013JD020905, 2014.
- 442 Lawrence, D. M., Oleson, K. W., Flanner, M. G., Thornton, P. E., Swenson, S. C., Lawrence, P. J., Zeng, X. B.,  
443 Yang, Z. L., Levis, S., Sakaguchi, K., Bonan, G. B., and Slater, A. G.: Parameterization Improvements and  
444 Functional and Structural Advances in Version 4 of the Community Land Model, *J Adv Model Earth Sy*, 3,  
445 M03001, doi:10.1029/2011ms000045, 2011.
- 446 Lombardozzi, D., Sparks, J. P., Bonan, G., and Levis, S.: Ozone exposure causes a decoupling of conductance  
447 and photosynthesis: implications for the Ball-Berry stomatal conductance model, *Oecologia*, 169, 651-659,  
448 doi:10.1007/s00442-011-2242-3, 2012.
- 449 Lombardozzi, D., Sparks, J. P., and Bonan, G.: Integrating O-3 influences on terrestrial processes:  
450 photosynthetic and stomatal response data available for regional and global modeling, *Biogeosciences*, 10,  
451 6815-6831, doi:10.5194/bg-10-6815-2013, 2013.
- 452 Lombardozzi, D., Levis, S., Bonan, G., Hess, P. G., and Sparks, J. P.: The Influence of Chronic Ozone Exposure  
453 on Global Carbon and Water Cycles, *J Climate*, 28, 292-305, doi:10.1175/JCLI-D-14-00223.1, 2015.
- 454 Marengo, A., Gouget, H., Nedelec, P., Pages, J. P., and Karcher, F.: Evidence of a Long-Term Increase in  
455 Tropospheric Ozone from Pic Du Midi Data Series - Consequences - Positive Radiative Forcing, *J Geophys*  
456 *Res-Atmos*, 99, 16617-16632, doi:10.1029/94jd00021, 1994.
- 457 Neale, R. B., Richter, J., Park, S., Lauritzen, P. H., Vavrus, S. J., Rasch, P. J., and Zhang, M. H.: The Mean  
458 Climate of the Community Atmosphere Model (CAM4) in Forced SST and Fully Coupled Experiments, *J*  
459 *Climate*, 26, 5150-5168, doi:10.1175/JCLI-D-12-00236.1, 2013.
- 460 Oleson, K. W., Lawrence, D. M., Gordon, B., Flanner, M. G., Kluzek, E., Peter, J., Levis, S., Swenson, S. C.,  
461 Thornton, E., and Feddema, J.: Technical description of version 4.0 of the Community Land Model (CLM),  
462 2010.
- 463 Pacifico, F., Folberth, G. A., Sitch, S., Haywood, J. M., Rizzo, L. V., Malavelle, F. F., and Artaxo, P.: Biomass  
464 burning related ozone damage on vegetation over the Amazon forest: a model sensitivity study, *Atmos Chem*  
465 *Phys*, 15, 2791-2804, doi:10.5194/acp-15-2791-2015, 2015.
- 466 Parrish, D. D., Lamarque, J. F., Naik, V., Horowitz, L., Shindell, D. T., Staehelin, J., ... & Gilge, S. (2014).  
467 Long-term changes in lower tropospheric baseline ozone concentrations: Comparing chemistry-climate models  
468 and observations at northern midlatitudes. *Journal of Geophysical Research: Atmospheres*, 119(9), 5719-5736,  
469 doi: 10.1002/2013JD021435, 2014.
- 470 Sitch, S., Cox, P. M., Collins, W. J., and Huntingford, C.: Indirect radiative forcing of climate change through  
471 ozone effects on the land-carbon sink, *Nature*, 448, 791-U794, doi:10.1038/nature06059, 2007.
- 472 Sun, Y., Gu, L. H., and Dickinson, R. E.: A numerical issue in calculating the coupled carbon and water fluxes  
473 in a climate model, *J Geophys Res-Atmos*, 117, D22103, doi:10.1029/2012jd018059, 2012.



- 474 Tai, A. P. K., Mickley, L. J., Heald, C. L., and Wu, S. L.: Effect of CO<sub>2</sub> inhibition on biogenic isoprene  
475 emission: Implications for air quality under 2000 to 2050 changes in climate, vegetation, and land use, *Geophys*  
476 *Res Lett*, 40, 3479-3483, doi:10.1002/grl.50650, 2013.
- 477 Val Martin, M., Heald, C. L., & Arnold, S. R. (2014). Coupling dry deposition to vegetation phenology in the  
478 Community Earth System Model: Implications for the simulation of surface O<sub>3</sub>. *Geophysical Research Letters*,  
479 41(8), 2988-2996, doi:10.1002/2014GL059651, 2014.
- 480 Val Martin, M., Heald, C. L., Lamarque, J. F., Tilmes, S., Emmons, L. K., & Schichtel, B. A. (2015). How  
481 emissions, climate, and land use change will impact mid-century air quality over the United States: a focus on  
482 effects at national parks. *Atmos. Chem. Phys*, 15, 2805-2823.
- 483 Wittig, V. E., Ainsworth, E. A., and Long, S. P.: To what extent do current and projected increases in surface  
484 ozone affect photosynthesis and stomatal conductance of trees? A meta-analytic review of the last 3 decades of  
485 experiments, *Plant Cell Environ*, 30, 1150-1162, doi:10.1111/j.1365-3040.2007.01717.x, 2007.
- 486 Wu, S., Mickley, L. J., Kaplan, J. O., and Jacob, D. J.: Impacts of changes in land use and land cover on  
487 atmospheric chemistry and air quality over the 21st century, *Atmos Chem Phys*, 12, 1597-1609,  
488 doi:10.5194/acp-12-1597-2012, 2012.
- 489 Yue, X., and Unger, N.: Ozone vegetation damage effects on gross primary productivity in the United States,  
490 *Atmos Chem Phys*, 14, 9137-9153, doi:10.5194/acp-14-9137-2014, 2014.
- 491 Yue, X., and Unger, N.: The Yale Interactive terrestrial Biosphere model version 1.0: description, evaluation  
492 and implementation into NASA GISS ModelE2, *Geosci Model Dev*, 8, 2399-2417, doi:10.5194/gmd-8-2399-  
493 2015, 2015.
- 494

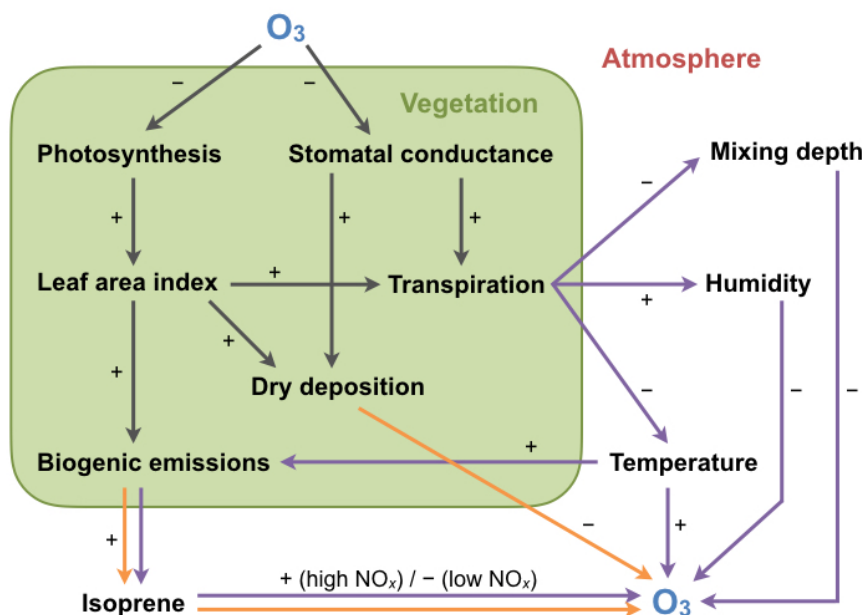


495 Table 1. Slopes (per  $\text{mmol m}^{-2}$ ) and intercepts (unitless) used to calculate ozone impact  
496 factors in Eq. (4) and (5), following Lombardozzi et al. (2015).  
497

| Plant group          | Photosynthesis  |                     | Conductance     |                     |
|----------------------|-----------------|---------------------|-----------------|---------------------|
|                      | Slope ( $a_p$ ) | Intercept ( $b_p$ ) | Slope ( $a_c$ ) | Intercept ( $b_c$ ) |
| Broadleaf            | 0               | 0.8752              | 0               | 0.9125              |
| Needleleaf           | 0               | 0.839               | 0.0048          | 0.7823              |
| Crops and<br>grasses | -0.0009         | 0.8021              | 0               | 0.7511              |

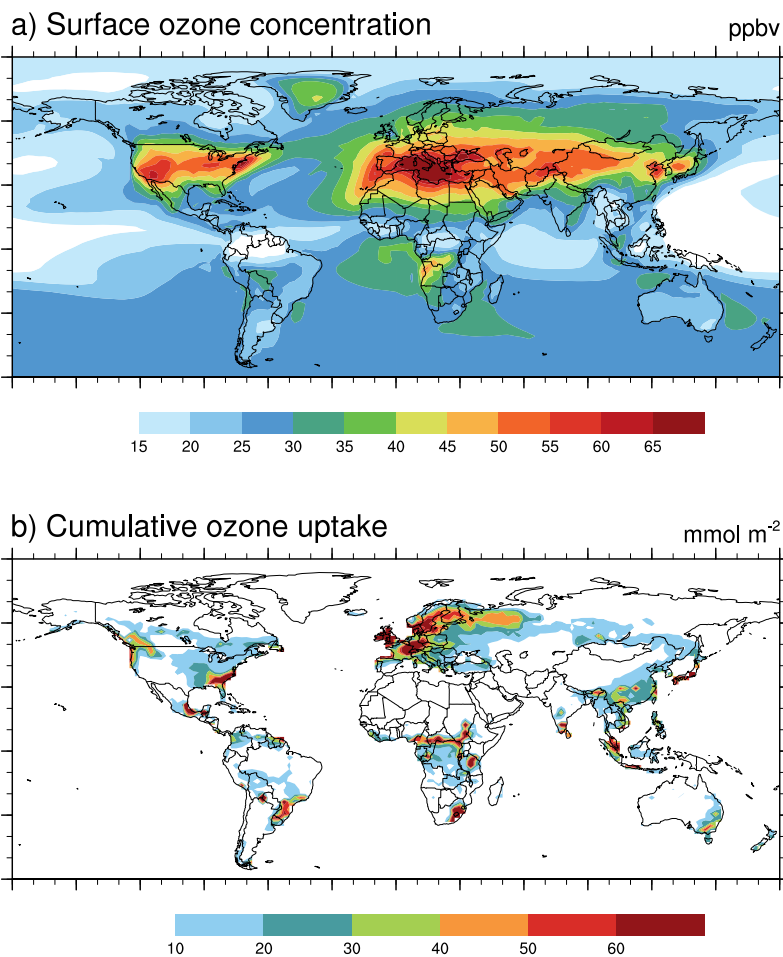
498

499



500  
 501  
 502  
 503  
 504  
 505  
 506

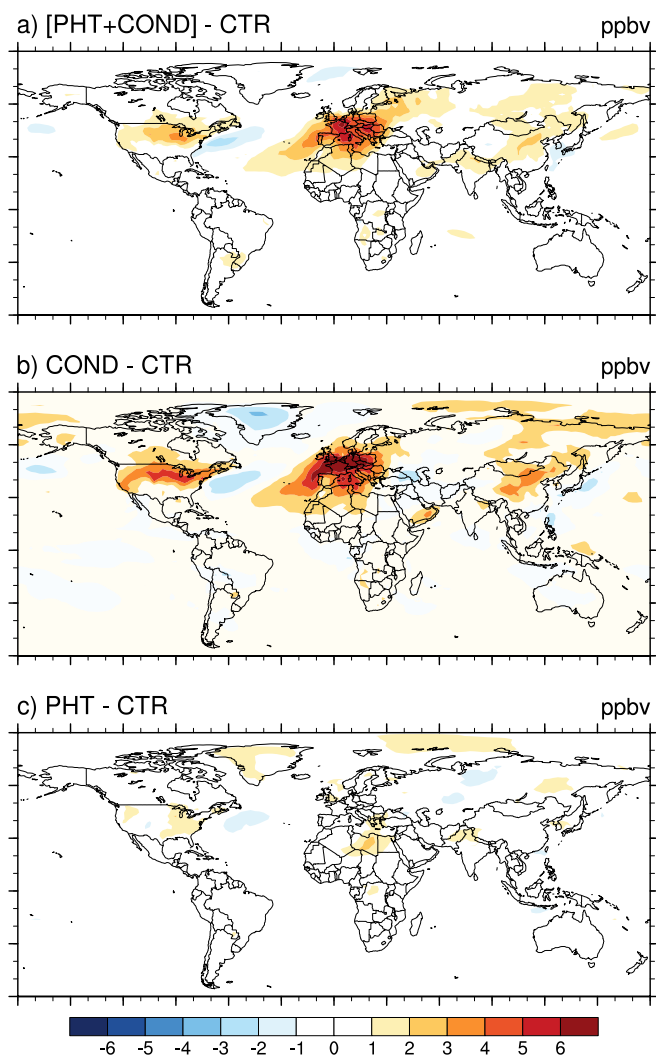
Figure 1. Possible pathways of ozone-vegetation coupling and feedbacks. The sign on each arrow indicates the sign of correlation or effect of one variable with or on another variable; the product of all signs along a given pathway indicates the overall sign of feedback. Orange arrows indicate biogeochemical feedbacks (i.e., via modulating atmospheric chemistry directly); purple arrows indicate meteorological feedbacks (i.e., via modifying the meteorological environment). We focus only on processes that directly affect ozone; meteorological feedbacks on photosynthesis and stomatal conductance are included in the model but not emphasized in this figure.



507

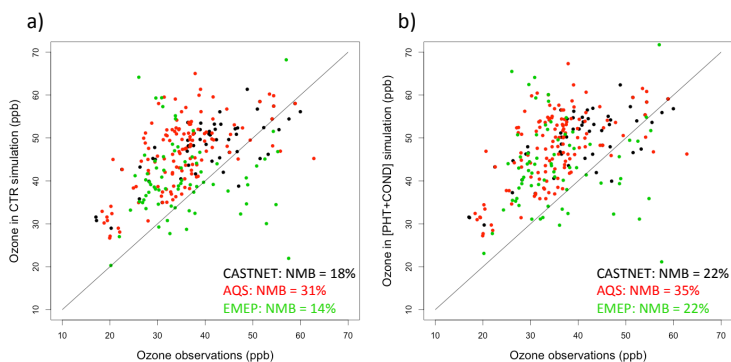
508 Figure 2. (a) Mean summertime (JJA) surface ozone concentration and (b) cumulative ozone uptake (CUO) from the  
509 [PHT+COND] case, where ozone uptake simultaneously modifies both photosynthetic rate and stomatal conductance.  
510 Results are averaged over the last 15 years of simulations.





511

512 Figure 3. Changes in summertime surface ozone concentrations in different simulations: (a) the case where both  
513 photosynthetic rate and stomatal conductance are modified by ozone uptake; (b) modified photosynthetic rate only; and (c)  
514 modified stomatal conductance only, all relative to the control case (CTR).



515

516

Figure 4. Scatterplots of simulated summertime ozone concentration in (a) the control case (CTR); and (b) the case where

517

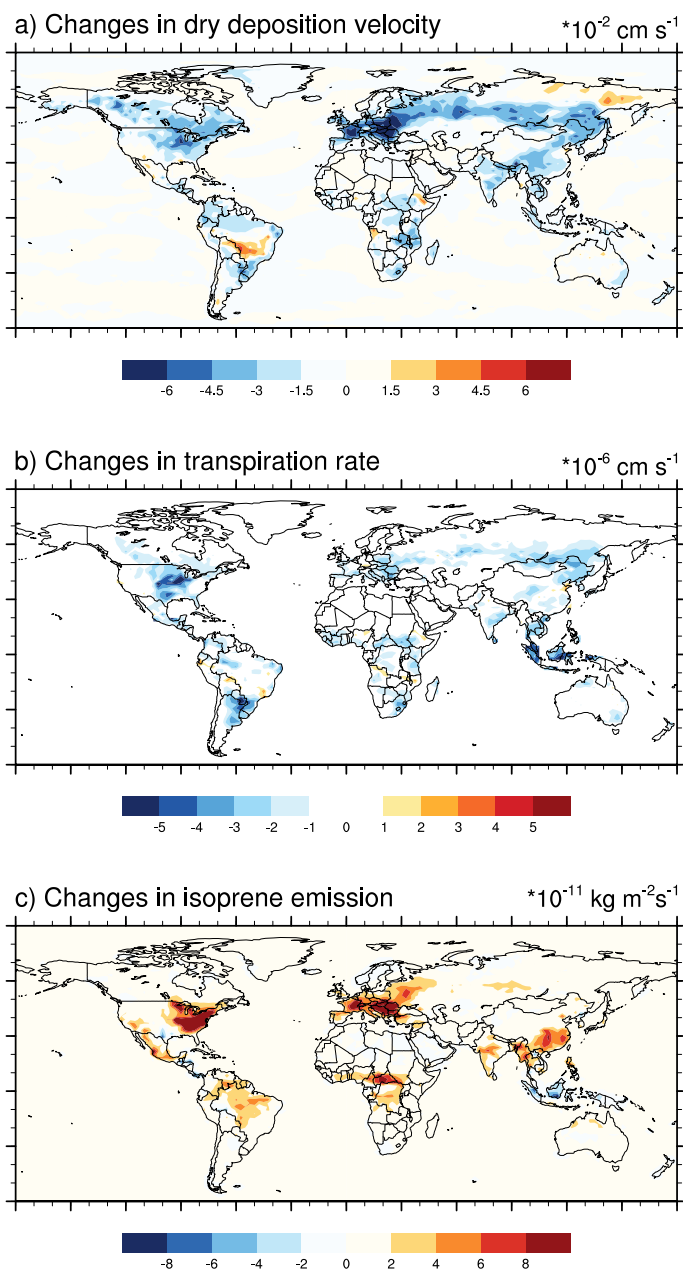
both photosynthesis and conductance are modified by ozone uptake ([PHT+COND]), versus observed average values from

518

the Clean Air Status and Trends Network (CASTNET) (1999-2001), Air Quality System (AQS) (1999-2001), and European

519

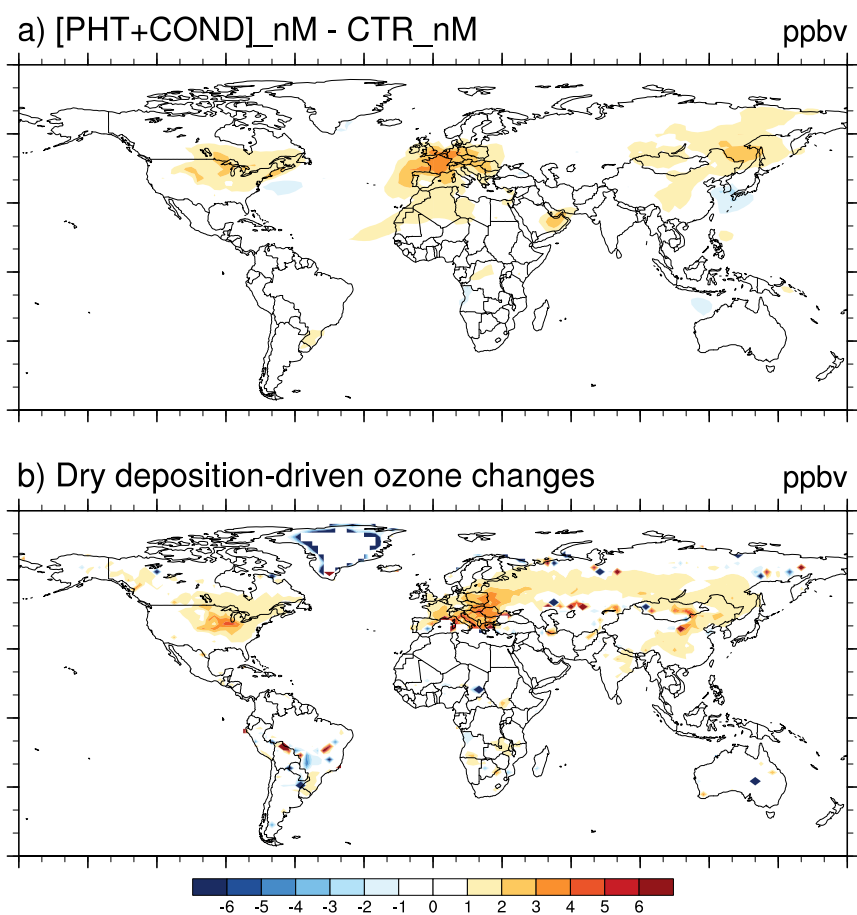
Monitoring and Evaluation Programme (EMEP) (1999-2001). Normalized mean biases (NMB) are also shown.



520

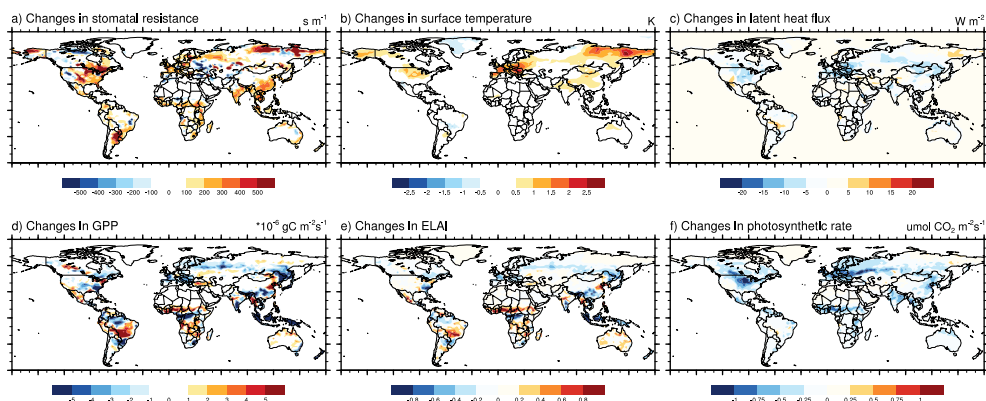
521 Figure 5. Changes in (a) dry deposition velocity, (b) transpiration rate and (c) isoprene emission in the [PHT+COND] case,

522 where both photosynthetic rate and stomatal conductance are modified by ozone uptake, relative to the control case (CTR).



523

524 Figure 6. Changes in surface ozone concentration in: (a) the case where both photosynthesis and stomatal conductance are  
525 modified by ozone uptake, but with prescribed isoprene emission from the original control case (CTR) by turning off  
526 MEGAN; and (b) theoretical changes calculated by multiplying our simulated dry deposition changes with the change in  
527 ozone concentration per unit change in dry deposition from Val Martin et al. (2014), which did not include ozone damage on  
528 vegetation.



529

530 Figure 7. Changes in (a) stomatal resistance, (b) surface temperature, (c) latent heat flux, (d) gross primary production

531 (GPP), (e) effective leaf area index (ELAI) and (f) photosynthetic rate in the [PHT+COND] case, where both photosynthetic

532 rate and stomatal conductance are modified by ozone uptake, relative to the control case (CTR).